

Reversible effect of hydrogen on superconductivity and weak ferromagnetism in $\text{Eu}_{1.4}\text{Ce}_{0.6}M\text{Sr}_2\text{Cu}_2\text{O}_{10-\delta}$ ($M=\text{Nb}$ and Ru)

I. Felner and U. Asaf

Racah Institute of Physics, The Hebrew University, Jerusalem, 91904, Israel

S. D. Goren and C. Korn

Department of Physics, Ben-Gurion University, Beer-Sheva 84105, Israel

(Received 21 April 1997; revised manuscript received 4 June 1997)

We have investigated the superconducting compounds $\text{Eu}_{1.4}\text{Ce}_{0.6}M\text{Sr}_2\text{Cu}_2\text{O}_{10-\delta}$ ($M=\text{Nb}$ and Ru) ($T_c=22$ and 32 K, respectively), as well as these materials charged with hydrogen, by several complementary experimental techniques. $\text{Eu}_{1.4}\text{Ce}_{0.6}\text{RuSr}_2\text{Cu}_2\text{O}_{10-\delta}$ is magnetically ordered at $T_N=122$ K, thus $T_N \gg T_c$. Superconductivity (SC) is confined to the CuO_2 planes, and the magnetic ordering is due to the Ru sublattice. Among many interesting features, irreversibility phenomena at low magnetic fields and a magnetic spin reorientation transition, which are observed, originate from antisymmetric exchange coupling of the Dzyaloshinsky-Moria type. The effect of hydrogen (0.35 at. %) is to suppress SC in both compounds and to enhance the weak-ferromagnetic properties of the Ru sublattice ($T_N=225$ K). In contrast to other high- T_c materials, this effect is reversible: namely, by depletion of hydrogen, SC is restored in both materials and for $M=\text{Ru}$, the T_N drops back to 122 K. [S0163-1829(98)03001-X]

INTRODUCTION

The interaction of hydrogen with high- T_c materials has been studied by many groups in the past and a large amount of data are available.¹⁻⁴ There is general agreement that hydrogen reduces the number of charge carriers in p -type high- T_c samples, and that the materials become semiconducting and magnetic at high hydrogen concentrations. We have shown that in $\text{YBa}_2\text{Cu}_3\text{O}_7\text{H}_y$, superconductivity (SC) is suppressed for $y=1.3$ (Ref. 1) and the Cu(2) sites become anti-ferromagnetically ordered at $T_N=420$ K, in a way very similar to that caused by removal of oxygen, e.g., $\text{YBa}_2\text{Cu}_3\text{O}_6$. On the other hand, in $\text{YBa}_2\text{Cu}_4\text{O}_8\text{H}_y$, (124) T_c is unaffected by hydrogen charging (up to $y=1.85$), but the shielding fraction is reduced sharply with an increasing in y .² Hydrogen induces a magnetic order in this system that leads to a phase separation: superconducting and magnetic. Their relative amount depends on the hydrogen concentration.

Much attention has been focused on a phase resembling the SC $\text{YBa}_2\text{Cu}_3\text{O}_7$ (YBCO) materials having the composition $R_{1.5}\text{Ce}_{0.5}M\text{Sr}_2\text{Cu}_2\text{O}_{10}$ (denoted as M -2122, $R=\text{Sm}$, Eu , or Gd and $M=\text{Nb}$, Ru , or Ta).⁵⁻⁹ The tetragonal (space group $I4/mmm$) M -2122 structure evolves from the YBCO structure by inserting fluorite type $R_{1.5}\text{Ce}_{0.5}\text{O}_2$ layers (instead of the Y layer in YBCO), thus shifting alternate perovskite blocks by $(a+b/2)$. The M ions reside in the Cu(1) site and only one distinct Cu site [corresponding to Cu(2)] exists with fivefold pyramidal coordination. The CuO_2 layers are separated on one side by MO_6 , which replaces the Cu-O chains, and on the other side by $R_{1.5}\text{Ce}_{0.5}\text{O}_2$ layers. The hole doping of the Cu-O planes, with resulting metallic behavior and SC, can be achieved with appropriate variation of the R/Ce ratio. The Nb-2122 are SC with $T_c \sim 22$ K, independent of R ,⁶⁻⁸ and it was recently shown that the Ru-2122 compounds^{5,10} are also SC with T_c up to 42 K. In addition, the latter system

is magnetically ordered, with T_N up to 180 K and our Mössbauer spectroscopy studies on ⁵⁷Fe-doped samples indicate clearly that the weak-ferromagnetic (WFM) state is confined to the Ru site.

The coexistence or mutual exclusion of SC and long-range magnetic order is one of the fundamental problems of condensed matter physics and has been studied experimentally and theoretically for almost four decades. This field was strongly revived in the early 1980s by the discovery of ternary intermetallic systems such as RRh_4B_4 , RMO_6S_8 ,¹¹ and more recently by the discovery of $\text{RNi}_2\text{B}_2\text{C}$,¹² where transition-metal elements responsible for SC and the magnetic rare-earth ions occupy different regular sublattices. The relatively weak interaction between the transition-metal d electrons and the localized f shells, resulting from complete separation in space, permits both phenomena to coexist, and the trend is that for *all* the intermetallic magnetic superconductors, the magnetic ordering is well below the onset of SC ($T_N < T_c$). The coexistence of bulk SC in the WFM state in the ceramic Ru-2122 system indicates that this system belongs to the same class of magnetic superconductors as do the intermetallics. However, in contrast to the intermetallic systems, in the Ru-2122 system, the WFM ordering is well above the SC state ($T_N/T_c > 4$).⁵

In attempting to understand the mechanism of SC and WFM in $\text{Eu}_{1.4}\text{Ce}_{0.6}M\text{Sr}_2\text{Cu}_2\text{O}_{10-\delta}$ ($M=\text{Nb}$ and Ru), an approach involving reducing the number of charge carriers by hydrogen charging was employed. Similar to other high-temperature superconducting (HTSC) materials, we show that 0.35 at. % of hydrogen suppresses SC in both materials. In addition, in the magnetic superconductor $\text{Eu}_{1.4}\text{Ce}_{0.6}\text{RuSr}_2\text{Cu}_2\text{O}_{10-\delta}$ (EuCeRu) all the magnetic properties and the irreversible phenomena of the magnetic state (T_N , the coercive fields, the remanent moments, etc.) are enhanced. The main subject addressed here is that both the

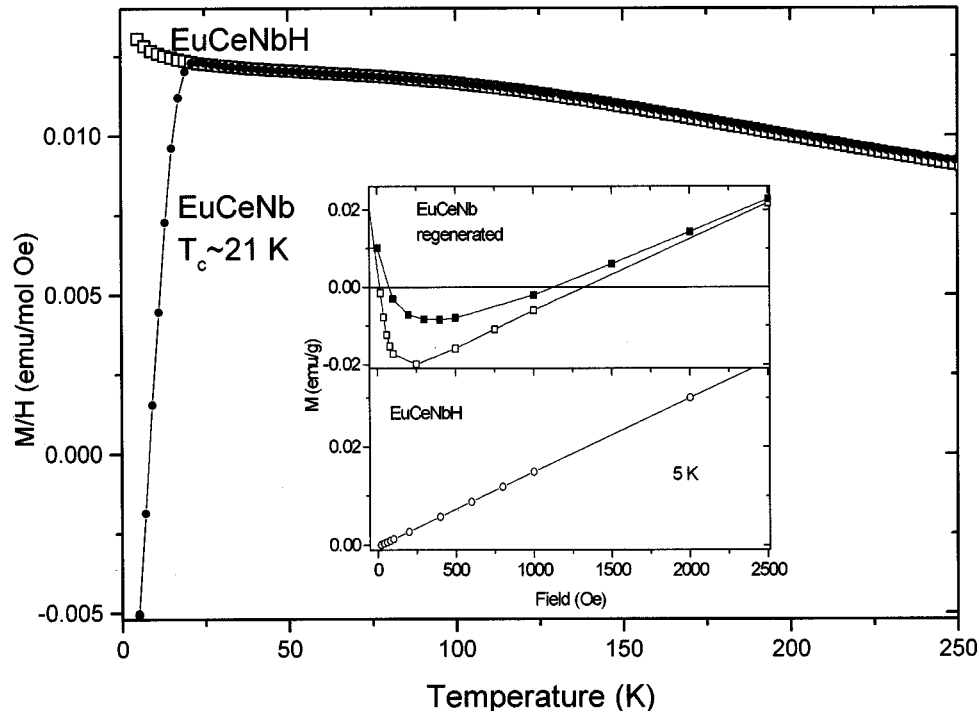


FIG. 1. Temperature dependence of the magnetic susceptibility measured at 1 kOe for $\text{Eu}_{1.4}\text{Ce}_{0.6}\text{NbSr}_2\text{Cu}_2\text{O}_{10-\delta}$ and 0.35 at. % hydrogen charged in $\text{Eu}_{1.4}\text{Ce}_{0.6}\text{NbSr}_2\text{Cu}_2\text{O}_{10-\delta}$. The isothermal magnetization curves at 5 K for the EuCeNbH and the regenerated samples are shown in the inset.

suppression of SC and the enhancement of antiferromagnetism (AFM) are reversible. We show that by removal of hydrogen, SC is restored in both materials and for EuCeRu the magnetic properties of the uncharged sample are recovered. This is in contrast to the behavior observed in all other HTSC materials, in which charging and/or depletion of hydrogen is irreversible and destructive.³

EXPERIMENTAL DETAILS

Ceramic samples with nominal composition $\text{Eu}_{1.4}\text{Ce}_{0.6}M\text{Sr}_2\text{Cu}_2\text{O}_{10}$ were prepared by a solid state reaction technique. Prescribed amounts of Eu_2O_3 , CeO_2 , SrCO_3 , Ru , Nb_2O_5 , and CuO were mixed and pressed into pellets and preheated at 1000 °C for about 1 day in the presence of flowing oxygen at atmospheric pressure. The products were cooled, reground, and sintered at 1050 or 1120 °C (for $M = \text{Ru}$ or Nb) for 72 h in a slightly pressurized oxygen (about 1.4 atm) and then furnace cooled to ambient temperature. Powder x-ray-diffraction (XRD) measurements confirmed the purity of the compounds ($\sim 97\%$) and indicate that all materials have tetragonal-type structure. Hydrogen absorption was accomplished by direct contact with hydrogen gas at 100 °C in a fixed volume and the amount of hydrogen absorbed was determined by noting the change in gas pressure. Samples with one concentration [0.35(2) at. %] were studied. To remove the hydrogen, a part of each hydrogenated sample was reheated for 10 h at 250 °C under ambient pressure. These materials are denoted as the "regenerated samples."

The dc magnetic measurements on solid ceramic pieces (on powdered sample for the regenerated samples) in the range of 2–300 K were performed in a commercial (Quan-

tum Design) superconducting quantum interference device magnetometer (SQUID). The magnetization was measured by two different procedures. (a) The sample was zero field cooled (ZFC) to 5 K, a field was applied and the magnetization was measured as a function of temperature. (b) The sample was field cooled (FC) from above 250 K to 5 K and the magnetization was measured. The Mossbauer spectroscopy studies (MS) of ^{151}Eu were carried out using a conventional constant acceleration spectrometer and a 50 mCi $^{151}\text{SmF}_3$ source, and the isomer shifts (IS) are reported with respect to this source.

EXPERIMENTAL RESULTS

XRD studies show that $\text{Eu}_{1.4}\text{Ce}_{0.6}M\text{Sr}_2\text{Cu}_2\text{O}_{10-\delta}$ ($M = \text{Nb}$ and Ru) has a tetragonal structure with the space group $I4/mmm$. The lattice parameters are $a = 3.866(1)$, $3.846(1)$ Å and $c = 28.72(1)$, $28.50(1)$ Å, respectively. These lattice parameters are in excellent agreement with data published in Refs. 8–10. In the limit of uncertainty, the hydrogen charged samples have the same size as the parent compound. MS performed at 90 and 300 K on ^{151}Eu in the two host and hydrogen loaded materials (not shown) show a single narrow linewidth in the range of 2.48(1)–2.27(1) mm/s. The fit yields IS of 0.67(2) mm/s and a quadrupole splitting in the range of 2.20–2.52 mm/s. The small IS values obtained indicate that in all samples the Eu ions are trivalent with a nonmagnetic $J=0$ ground state. Roughly speaking, the MS values obtained are not sensitive to the M ions or to whether the samples are hydrogen loaded. In the subsequent figures, unless otherwise specified, the susceptibility in units of emu/mol Oe is defined as the ratio of the magnetization M to the applied field H ($\chi = M/H$).

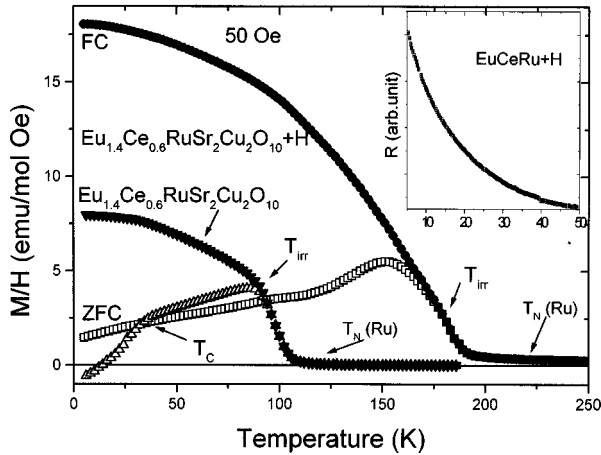


FIG. 2. Temperature dependence of the magnetic susceptibility measured at 50 Oe for $\text{Eu}_{1.4}\text{Ce}_{0.6}\text{RuSr}_2\text{Cu}_2\text{O}_{10-\delta}$ and 0.35 at. % hydrogen charged in $\text{Eu}_{1.4}\text{Ce}_{0.6}\text{RuSr}_2\text{Cu}_2\text{O}_{10-\delta}$. Temperature dependence of the resistivity in arbitrary unit for $\text{EuCeRu}+\text{H}$ is shown in the inset.

A. The effect of hydrogen on the SC $\text{Eu}_{1.4}\text{Ce}_{0.6}\text{NbSr}_2\text{Cu}_2\text{O}_{10-\delta}$

Magnetic susceptibility studies (Fig. 1) of $\text{Eu}_{1.4}\text{Ce}_{0.6}\text{NbSr}_2\text{Cu}_2\text{O}_{10-\delta}$ (EuCeNb) measured at 1 kOe show an onset of SC at $T_c=21(1)$ K, in good agreement with Ref. 7. For the hydrogen charged sample (EuCeNbH) SC is totally suppressed and the nearly linear isothermal positive $M(H)$ curve clearly indicates a normal paramagnetic behavior. (Fig. 1 inset). Note the merging of $\chi(T)$ curves above T_c .

Previous thermogravimetric analysis indicates⁷ that the Nb-1222 system is stable up to 600 °C and no oxygen weight loss is detected. Therefore, it is assumed that in the “regenerated” EuCeNb sample only the absorbed hydrogen is depleted, and no oxygen gain is involved. Our magnetic mea-

surements show that for the “regenerated” sample, SC is restored with $T_c=21$ K. $M(H)$ measurements at 5 K for this material (Fig. 1 inset) exhibit the typical hysteresis loop for a SC compound. The diamagnetic signal increases linearly up to 90 Oe, and the estimated shielding fraction deduced from this curve is $\sim 20\%$, indicating bulk SC. Therefore, we may conclude with high confidence that the suppression of SC by hydrogen loading is reversible, and by removal of hydrogen SC is restored. This is definitely in contrast to the behavior observed in all other HTSC materials, in which charging of hydrogen is irreversible and destructive.³

B. The effect of hydrogen on the SC and magnetic behavior of $\text{Eu}_{1.4}\text{Ce}_{0.6}\text{RuSr}_2\text{Cu}_2\text{O}_{10-\delta}$

Our main interest here is to compare the magnetic properties of EuCeRu (Ref. 5) and the hydrogen loaded $\text{EuCeRu}+\text{H}$ materials. For the sake of clarity, we shall refer briefly to magnetic studies of EuCeRu where SC occurs for Ce contents of 0.5–0.8, but the highest T_c was obtained for $x=0.6$,¹⁰ the concentration that has been studied here.

The magnetization curves in EuCeRu are composed of three contributions: (a) a negative moment below T_c due to a SC state, (b) a positive moment due to the paramagnetic effective moment of Eu and (c), a contribution from the ferromagneticlike behavior of the Ru sublattice. ZFC and FC magnetic measurements were performed for a broad range of field strengths, and typical $\chi(T)$ curves measured at $H=50$ Oe are shown in Fig. 2. The ZFC branch at low temperatures is negative, and $T_c=32$ K, obtained from resistivity measurements⁵ can be also observed from this curve. Since SC is confined to the CuO_2 planes, all the magnetic anomalies in Fig. 2 above T_c are related to the Ru-O planes. The two ZFC and FC curves merge at $T_{\text{irr}}=92$ K. T_{irr} decreases with field and around $H=2$ kOe the irreversibility is washed out.⁵ Note that $T_N(\text{Ru})$ is not at T_{irr} . The $\chi(T)$

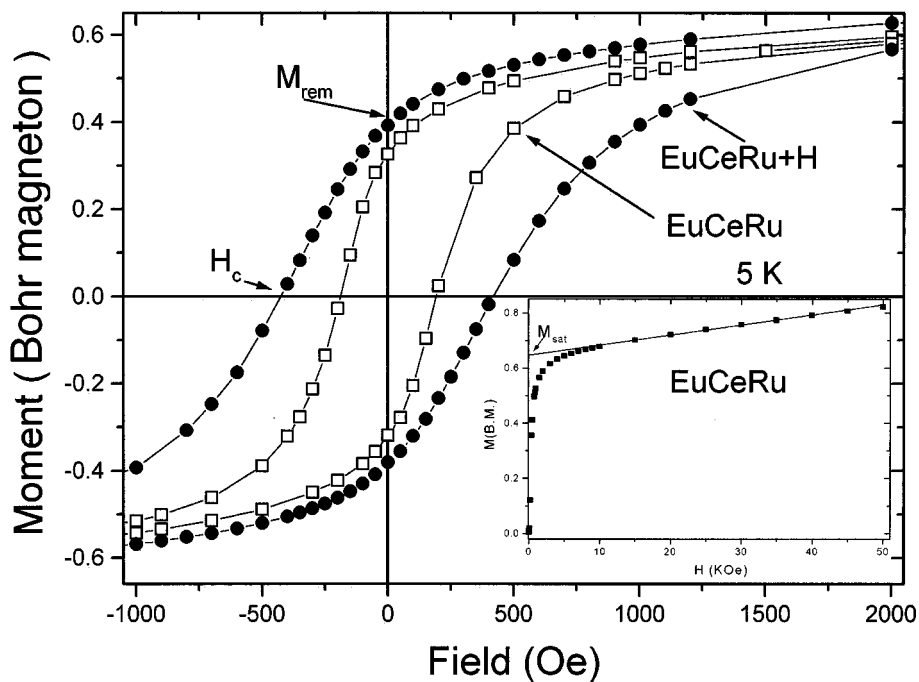


FIG. 3. Hysteresis loops at 5 K for EuCeRu and $\text{EuCeRu}+\text{H}$. The inset extends the $M(H)$ curve for EuCeRu up to 50 kOe.

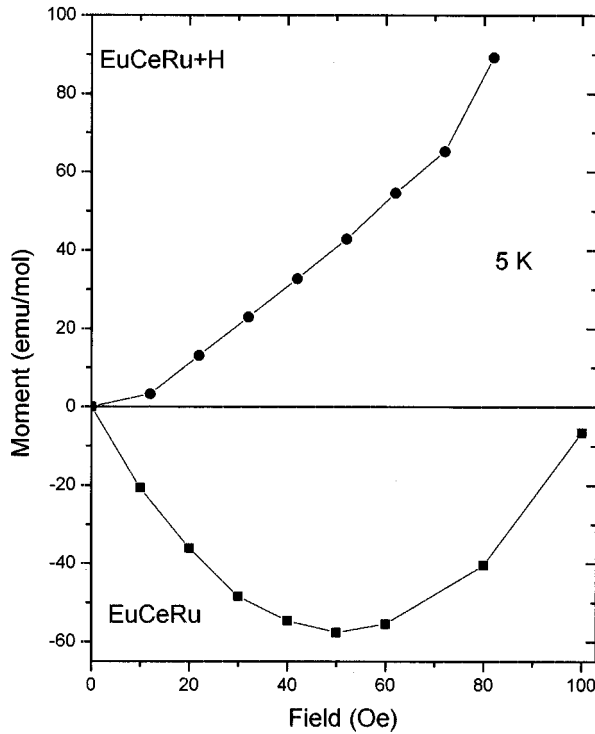


FIG. 4. Virgin magnetization curves at 5 K for EuCeRu and EuCeRu+H. Note the negative values for the SC EuCeRu and the peak at 50 Oe.

curves in Fig. 2 do not lend themselves to an easy determination of T_N (Ru), and T_N (Ru)=122 K was obtained from ac $\chi(T)$ measurements,⁵ and directly from the temperature dependence of the saturation moment (Fig. 5) discussed later. No other anomalies were observed at higher temperatures. The irreversibility at T_{irr} arises as a result of an anti-symmetric exchange coupling of the Dzyaloshinsky-Moriya (DM) type¹³ between neighboring Ru moments, induced by a local distortion that breaks the tetragonal symmetry of the RuO₆ octahedra. Due to this DM interaction, the field causes the adjacent spins to cant slightly out of their original direction and to align a component of the moments with the direction of H . Below T_{irr} the Ru-Ru interactions begin to

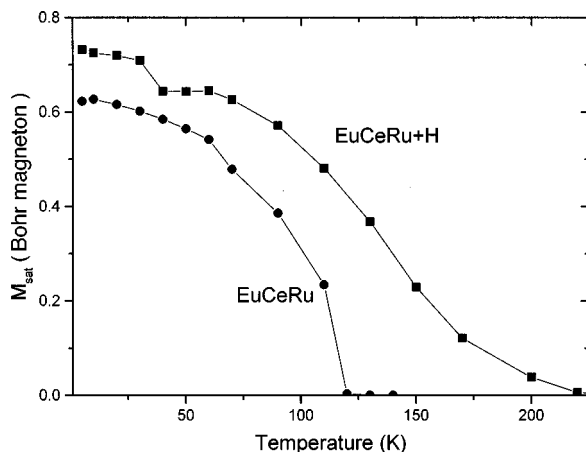


FIG. 5. Temperature dependence of the saturated magnetization M_{sat} for EuCeRu and EuCeRu+H. For both systems M_{sat} disappears at T_N (Ru).

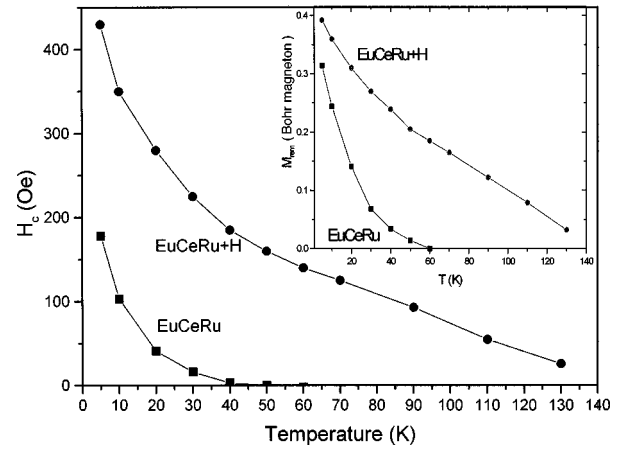


FIG. 6. Temperature dependence of the coercive fields, and remanent magnetization M_{rem} (inset) for EuCeRu and EuCeRu+H.

dominate, leading to reorientation of the Ru moments, and the peak in the ZFC branch is observed. The exact nature of the local structural distortions causing this reorientation is not presently known. Above T_N (Ru), the $\chi(T)$ curves adhere to the Curie-Weiss law.

$M(H)$ measurements at various temperatures for EuCeRu have been carried out, and at low temperatures, both the WFM and the SC properties are clearly observed in the curves (Figs. 3 and 4). At 5 K, (a) the negative moments increase linearly up to 30 Oe, typical for SC state below H_{C1} and (b) a hysteresis loop is opened below 1.5 kOe. The estimated shielding fraction deduced from this curve (ignoring possible contributions from Ru and/or Eu^{3+}) is about 30%, indicating bulk SC. Note that the $\chi(T)$ curves shown in Fig. 2 were measured in $H=50$ Oe where the highest negative signal in Fig. 4 is obtained. All $M(H)$ curves below $T_N = 122$ K are strongly dependent on the field up to about 2–3 kOe, until a common slope is reached. $M(H)$ can be described as $M(H) = M_{Ru} + \chi H$, where χH is the linear contribution of Eu^{3+} to M , and M_{Ru} which reaches its maximum (denoted as M_{sat}) at about 5 kOe, corresponds to the weak ferromagnetic component of the Ru sublattice. A typical curve for 5 K is exhibited in Fig. 3 (inset), and the value of $M_{sat} = 0.63(1) \mu_B$ obtained is much smaller than the fully saturated moment of $2 \mu_B$ expected for low-spin state of Ru^{4+} , i.e., $g \mu_B S$ for $g=2$ and $S=1$. This means that in the ordered state, a slight canting on adjacent Ru spins occurs. M_{sat} decreases with increasing of T , and becomes zero at T_N (Ru)=122(1) K (see Fig. 5). Two other characteristic parameters of the hysteresis loops are shown in Fig. 3; namely, the remanent moment (M_{rem}), and the coercive field (H_c). Both are also temperature dependent (Fig. 6). Surprisingly, H_c disappears at $T > T_c$, however, this is of little interest in our present paper and will be discussed elsewhere.¹⁴

The physical behavior of the hydrogen charged EuCeRu+H material is shown in Figs. 2–6. (a) The temperature dependence of the resistivity (in arbitrary units) shown in Fig. 2 (inset), (b) the absence of the deflection in the ZFC branch (Fig. 2), and (c) the positive $M(H)$ curve obtained at low fields (Fig. 4) all indicate clearly that in EuCeRu+H, SC is totally suppressed, and that this material behaves in a way similar to EuCeNbH (Fig. 1). Moreover, Figs. 2–6 exhibit the magnetic properties belonging to the Ru sites, which are

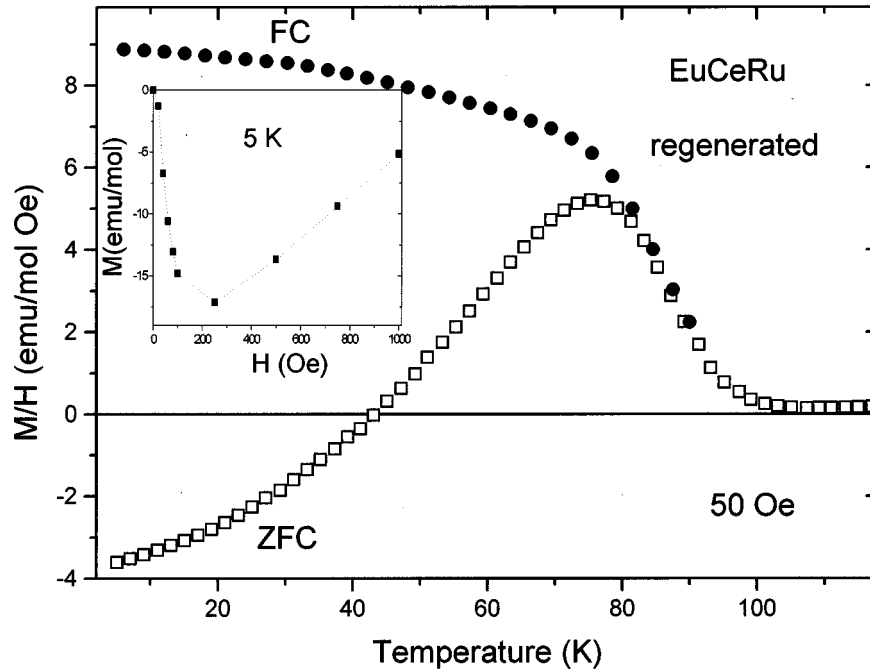


FIG. 7. Temperature dependence of the magnetic susceptibility measured at 50 Oe for the regenerated $\text{Eu}_{1.4}\text{Ce}_{0.6}\text{RuSr}_2\text{Cu}_2\text{O}_{10-\delta}$. Virgin magnetization curves at 5 K typical for a SC state, is shown in the inset.

all *enhanced*, as compared to the host EuCeRu. More specifically, the $\chi(T)$ values (at $H=50$ Oe) of the FC branch (Fig. 2) are much higher, and T_{irr} and $T_N(\text{Ru})$ are shifted to 167(2) and 225(2) K, respectively. The typical hysteresis loop at 5 K, opened below 5 kOe is much broader for EuCeRu+H (Fig. 3) and all the characteristic features such as M_{sat} , M_{rem} , and H_c extracted from the hysteresis loops measured at various temperatures and shown in Figs. 4–6 support this statement. Note the higher values and the discontinuity around 40 K in $M_{\text{sat}}(T)$ of EuCeRu+H (Fig. 5). The two $M_{\text{sat}}(T)$ curves show a different shape, thus scaling them is impossible. $T_N(\text{Ru})=225(2)$ K can be deduced directly from this curve. This indicates clearly that in EuCeRu the effect of hydrogen charging is to suppress SC, and to enhance the magnetic properties of the Ru sublattice.

C. SC and magnetic behavior of the regenerated

$\text{Eu}_{1.4}\text{Ce}_{0.6}\text{RuSr}_2\text{Cu}_2\text{O}_{10-\delta}$

Here again, we heated EuCeRu+H to 250 °C and assume that only the absorbed hydrogen is depleted. The ZFC and FC magnetic susceptibilities measured at 50 Oe of the regenerated EuCeRu (carried out on powdered sample) are shown in Fig. 7. Both the negative values in the ZFC branch at low temperatures, and the increase of the negative moments with the applied field at 5 K (Fig. 7 inset), indicate clearly that SC is restored for this sample; thus the suppression of SC by hydrogen is reversible. Note that (i) the ZFC branch becomes negative at around 40 K, and (ii) the peak in the $M(H)$ is shifted to 200 Oe, which indicates a higher T_c value for this material. Moreover, Fig. 7 shows that the two branches merge at $T_{\text{irr}} \sim 90$ K (in contrast to 167 K for EuCeRu+H) in perfect agreement with the T_{irr} of the parent sample (Fig. 2). The small difference in the M/H values (about 10%) between Fig. 2 and Fig. 7 is not significant, and probably arises from the fact that the dc magnetic measurements presented in

Fig. 2 were performed on solid ceramic piece, whereas for the regenerated material (Fig. 7) a fine powder has been used. In addition, there may be a positive contribution to the magnetization, due to the fact that a small remanent field exists in the SQUID magnetometer. This artificial contribution will affect mainly the magnetization values measured at low fields. $M(H)$ measurements for the regenerated sample at various temperatures and H up to 50 kOe have been performed, and some typical curves are shown in Fig. 8. Generally speaking, T_N observed is around 125 K [see the linear $M(H)$ at 150 K] and in the limit of uncertainty, the temperature dependence of M_{sat} for EuCeRu (shown in Fig. 5) is restored. Thus, all the “enhanced” parameters of EuCeRu+H presented in Figs. 2–6 are reduced to the original values of the parent EuCeRu compound.

The following experimental evidence *excludes* the possibility that the reversible magnetic behavior (Figs. 7 and 8) is an effect of change in the oxygen concentration. (1) As

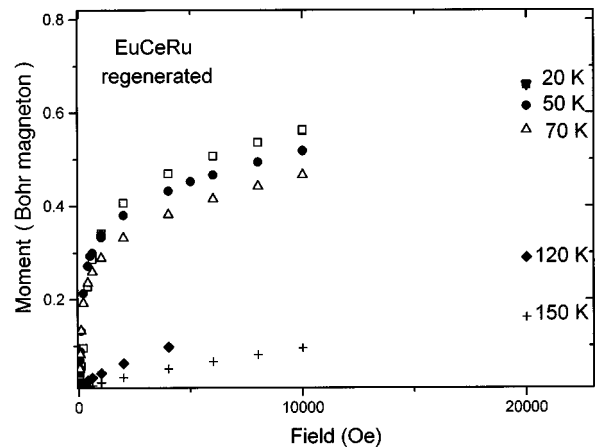


FIG. 8. Isothermal magnetization curves at various temperatures for regenerated EuCeRu. Note the linear $M(H)$ curve at 150 K.

stated above, previous thermogravimetric analysis indicates⁷ that the *M*-2122 system is stable up to 600 °C, and no oxygen weight loss is detected. Therefore, it is assumed that in the “regenerated” sample, where the heat treatments were performed at relative low temperatures (150–250 °C), only the absorbed hydrogen is depleted, and no oxygen gain is involved. (2) Our scanning-tunneling-spectroscopy studies show that the oxygen content of Ru-2122 samples treated at various temperatures and oxygen pressures remains constant up to 700 °C (to be published). (3) Samples annealed at 150 °C under vacuum for a few hours, exhibit similar magnetic behavior to the curves shown in Fig. 2 for the parent material.

DISCUSSION

The magnetic behavior of the hydrogen charged *M*-2122 (*M*=Nb and Ru) materials studied here can be compared to other ceramic SC systems such as YBCO and YBa₂Cu₄O₈, which have been studied extensively. As stated above, similar changes in the SC properties of YBCO can be induced by either removing oxygen or adding hydrogen, and the oxygen can be extracted easily. Two different reactions can take place with hydrogen. (a) At low hydrogen pressure, the extraction of oxygen leads to the formation of H₂O.³ (b) At high hydrogen pressure, a stable hydride is formed. In any case, hydrogen loading is a destructive reaction, and by heating the samples, hydrogen can be removed only as H₂O, the crystal structure is destroyed and SC is not restored.⁵

Hole (or carrier) density in the CuO₂ planes, or deviation of the formal Cu valence from Cu²⁺, is a primary parameter that governs *T_c* in most of the HTSC compounds. Chemically doped holes, which may be measured as the effective [CuO]^{*p*} charge (or the nominal Cu valence 2 + *p*), are obtained by depletion of oxygen in YBCO, or by increasing the Sr concentration in La_{2-*x*}Sr_{*x*}CuO₄. As already shown, SC emerges only in the narrow window of the carrier concentration; e.g., the highest *T_c* achieved for YBCO and La_{2-*x*}Sr_{*x*}CuO₄ is for *p*~0.2 and 0.15, respectively.¹⁵

The influence of hydrogen on EuCeNb and EuCeRu is reversible, which means that hydrogen loading is not destructive as in the YBCO and 124 systems. We assume that hydrogen resides in interstitial sites and changes the hole density of the SC CuO planes, either by increasing or decreasing the ideal effective charge *p* of the sample. Once *p* of the planes changes, SC is suppressed, and EuCeNbH and EuCeRu+H exhibit paramagnetic behavior down to 2 K. Depletion of hydrogen leads to the original *p* value and SC is restored.

The spin canting and the saturated magnetization (*M_{sat}*) in relatively low applied field are the striking features of EuCeRu. The isothermal magnetization curves, and the hys-

teresis loops at various temperatures expected for a WFM (Figs. 2 and 3) are quite obvious. The Ru spins (at 50 Oe) undergo a reorientation at *T_{irr}*=92 K, and at 2 kOe all the anomalies and the irreversibility in the $\chi(T)$ curves are washed out.⁵ More importantly, *M_{sat}*=0.63 μ_B Ru at 5 K is much smaller than 1.3 μ_B and 1.4 μ_B obtained for SrRuO₃ and Sr₃Ru₂O₇, respectively where simple charge counting leads to Ru⁴⁺. Indeed, $\chi(T)$ studies at elevated temperatures indicate that Ru⁴⁺ is in the low-spin *S*=1 state.¹⁶ Assuming similar valence of Ru in EuCeRu means that only a fraction of the Ru moments is aligned by the external field and saturates above 2 kOe. Although, EuCeRu exhibits normal paramagnetic behavior above *T_N*, the Ru ion valence cannot easily be determined, due to the following reasons. (1) The paramagnetic effective moment extracted is composed of two additional contributions: the high susceptibility of Eu³⁺, and that of Cu²⁺. (2) Determination of the absolute oxygen content is difficult, because CeO₂ and RuO₂ are not completely reducible⁷ to stoichiometric oxides on heating to high temperatures.

Hydrogenation enhances *T_N* and all other *weak* ferromagnetic characteristic features of the host EuCeRu material. This effect, which was also observed in several rare-earth-based intermetallic hydrides,¹⁷ is undoubtedly an electronic effect. As described above, in addition to the change in the hole density of the Cu-O planes, there is a transfer of electrons from H to the Ru 4*d* subbands, resulting in an increase in the moment of the Ru sublattice and hence to an increase in the overall magnetic parameters. An alternative way is to assume that the enhancement of *M_{sat}*, *M_{rem}*, and *H_c* arises from a change of the antisymmetric exchange coupling of the DM type between the adjacent Ru moments, which causes the spins to cant out of their original direction with a larger angle and as a result, a larger component of the Ru moments forms the WFM state. However, this scenario cannot reconcile the higher *T_N* observed in EuCeRu+H. The exact nature of the local structure distortions causing the WFM behavior in both materials, as well as the hydrogen location in the matrix, are not presently known and neutron diffraction studies are now being carried out to address these points. Our central assumption is that Ru in EuCeRu orders magnetically at elevated temperatures, and bulk SC is confined to the Cu-O planes, and both sublattices are practically decoupled. Since hydrogen loading affects both phenomena, and the original behavior is restored when hydrogen is depleted, we tend to believe that H atoms occupy interstitial sites close to these planes, presumably inside the Sr-O planes.

ACKNOWLEDGMENT

The research was supported by the Klachky Foundation for Superconductivity.

¹I. Felner, B. Brosh, S. D. Gorn, C. Corn, and V. Volterra, Phys. Rev. B **43**, 10 368 (1991).

²I. Felner, I. Nowik, B. Brosh, D. Hechel, and E. R. Bauminger, Phys. Rev. B **43**, 8737 (1991).

³H. Lutgemeier, S. Schmenn, H. Schone, Yu. Baikov, I.

Felner, S. Gorn, and C. Korn, J. Alloys Compd. **219**, 29 (1995).

⁴G. Dortmann, J. Erxmeyer, S. Blasser, J. Steiger, T. Poatsch, A. Weidinger, H. Karl, and B. Stritzker, Phys. Rev. B **49**, 600 (1994).

- ⁵I. Felner, U. Asaf, Y. Levi, and O. Millo, *Phys. Rev. B* **55**, R3374 (1997).
- ⁶I. Felner, D. Sprinzak, U. Asaf, and T. Kroner, *Phys. Rev. B* **51**, 3120 (1995).
- ⁷R. J. Cava, J. J. Krajewski, H. Takagi, H. W. Zandbergen, R. V. VanDover, W. F. Peck, Jr., and B. Hessen, *Physica C* **191**, 237 (1992); I. Felner, U. Yaron, U. Asaf, T. Kroner, and B. Breit, *Phys. Rev. B* **49**, 6903 (1994).
- ⁸T. J. Goodwin, H. B. Radousky, and R. N. Shelton, *Physica C* **204**, 212 (1993).
- ⁹M. Bennaahmias, H. B. Radousky, C. M. Buford, A. B. Kebede, M. McIntyre, T. J. Goodwin, and R. N. Shelton, *Phys. Rev. B* **53**, 2773 (1996).
- ¹⁰L. Bauernfeind, W. Widder, and H. F. Braun, *Physica C* **254**, 151 (1995).
- ¹¹For a review, L. N. Bulaevskii, A. I. Buzdin, M. I. Kubic, and S. V. Panjukov, *Adv. Phys.* **34**, 175 (1985).
- ¹²H. Eisaki, H. Takagi, R. J. Cava, B. Batlogg, J. J. Krajewski, W. F. Peck, Jr., K. Mizuhashi, T. O. Lee, and S. Uchida, *Phys. Rev. B* **50**, 647 (1994).
- ¹³J. Dzyaloshinsky, *J. Phys. Chem. Solids* **4**, 241 (1958); T. Moriya, *Phys. Rev.* **120**, 91 (1960).
- ¹⁴E. B. Sonin and I. Felner (unpublished)
- ¹⁵S. Uchida, *Physica C* **185-189**, 28 (1991).
- ¹⁶G. Cao, S. McCall, and J. E. Crow, *Phys. Rev. B* **55**, R672 (1997).
- ¹⁷L. Y. Zhang, G. T. Rado, S. H. Liou, and C. L. Chien, *J. Magn. Magn. Mater.* **62**, 203 (1986).